Tribology International 224 (2026) 112370

Contents lists available at ScienceDirect

Tribology International

journal homepage: www.elsevier.com/locate/triboint

Full Length Article

Mechanistic origins of pressure-regulated tribological reversal in periodically modulated DLC films

Naizhou Du [a,b], Xinlin Zhao [b], Xiaowei Li [a,b,f,**], Xubing Wei [b], Meng Cheng [b], Peng Guo [c], Rende Chen [c], Xinmeng Wu [d], Qiaoyun Dong [d], Weidong Dang [d,*], Kwang-Ryeol Lee [e], Aiying Wang [c,*]

[a] School of Chemical Engineering, China University of Mining and Technology, Xuzhou 221116, PR China
[b] School of Materials Science and Physics, China University of Mining and Technology, Xuzhou 221116, PR China
[c] State Key Laboratory of Advanced Marine Materials, Ningbo Institute of Materials Technology and Engineering, Chinese Academy of Sciences, Ningbo 315201, PR China
[d] Luxcase Precision Technology (Yancheng) Co., Ltd., Yancheng 224000, PR China
[e] Computational Science Center, Korea Institute of Science and Technology, Seoul 136-791, Republic of Korea
[f] Jiangsu Key Laboratory for 3C Products Additive Manufacturing and Surface Technology, Xuzhou 221116, PR China

ARTICLE INFO

Keywords:
Diamond-like carbon
Modulated multilayer
Friction mechanism
Molecular dynamics

ABSTRACT

Constructing the periodically modulated multilayer architectures is a prevalent strategy to resolve the intrinsic trade-off between hardness and stress in diamond-like carbon (DLC) films. However, the specific dynamic contributions of distinct modulated layers to structural evolution under complex loading remain elusive. Here, the structure-property relationships of modulated DLC films were investigated at the atomic scale, spanning from energetic deposition to dynamic tribology. A counterintuitive tribological reversal governed by pressure was identified, where increasing modulation period caused a degradation in frictional performance under moderate pressure but an enhancement under high pressure. The modulation period acted as a kinetic regulator governing competitive evolution pathways. In particular, under high-pressure conditions, frequent interfaces facilitated interfacial densification via energetic subplantation, transforming soft layers into a hard tribofilm that effectively supported loads through stress segmentation. Conversely, under lower pressures, shear stress was dominant, leading to the destabilization of thin layers and a consequent loss of load-bearing capacity. These findings establish a unified theoretical framework linking performance to a critical transition from shear-dominated softening to adaptive pressure-driven hardening, and thus provide essential criteria for tailoring coating architectures to specific operational contact pressures.

1. Introduction

Diamond-like carbon (DLC) films are widely employed as high-performance protective coatings in tribological systems due to their exceptional hardness, chemical inertness, and intrinsic self-lubricating properties [1–3]. Nevertheless, a fundamental paradox limits their broader industrial application [4,5]. Efforts to achieve higher hardness by increasing the fraction of sp^3-hybridized carbon typically result in excessive internal compressive stress, which in turn can cause poor adhesion or catastrophic delamination [6,7]. To overcome this constraint, a common engineering solution involves the construction of functionally graded or periodically modulated multilayer architectures. These systems incorporate soft (sp^2-rich) and hard (sp^3-rich) alternated layers, providing an effective strategy for decoupling mechanical hardness from internal stress [8–11]. For example, Wang et al. [12] successfully leveraged alternating tensile and compressive stress fields in Si-doped DLC multilayers to deposit ultra-thick films (>50 μm) with minimal residual stress (0.05 GPa).

Despite the prevalence of such modulated designs, a unified understanding of the optimal modulation period remains elusive. Experimental studies frequently reported conflicting trends regarding the influence of interface period on mechanical and tribological

* Corresponding authors.
** Corresponding author at: School of Materials Science and Physics, China University of Mining and Technology, Xuzhou 221116, PR China.
E-mail addresses: lixw0826@gmail.com, xwli@cumt.edu.cn (X. Li), dangweidong@163.com (W. Dang), aywang@nimte.ac.cn (A. Wang).

https://doi.org/10.1016/j.triboint.2026.112370
Received 12 May 2026; Received in revised form 5 June 2026; Accepted 20 June 2026
Available online 23 June 2026

performance [13–15]. For instance, Xu et al. [13] proposed that residual stress in soft/hard alternating DLC multilayers could be effectively mitigated by optimizing the modulation period. However, Usman et al. [15] reported a contradictory trend, wherein the stress was generally intensified with increasing the number of periods, only exhibiting a slight reduction in dual-period configurations, which was also accompanied by the aggravation of wear rate at high contact stress. These discrepancies largely stem from a lack of fundamental insight into the structure-property relationships at the atomic scale. It is impossible to predict whether increasing the number of modulation periods will act as a mechanism for stress relief or a source of structural discontinuity.

Moreover, the understanding of how alternating soft and hard layers evolve structurally during dynamic friction remains significantly fragmented. For instance, Lin et al. [14,16] utilized unbalanced magnetron sputtering to fabricate C/C multilayers and investigated their tribological performance under high contact pressure. Their results indicated that a specific hard-layer fraction (50%) provided optimal tribological properties, which was ascribed to the lubricating effect of the formed transfer film, highlighting the acute sensitivity of the tribological response to the properties of the outermost surface layers. However, the specific dynamic contributions of these distinct layers and the atomistic mechanisms governing their in-situ interaction remain obscure. Elucidating this dynamic evolution is pivotal not only for advancing the theoretical framework of modulation effects, but also for expanding the application scenarios of multilayer DLC architectures.

Hence, this study employs large-scale molecular dynamics (MD) simulations to comprehensively explore structural properties of DLC films with varying modulation periods, spanning from energetic deposition to static nanoindentation and dynamic tribology [17–20]. The investigation first elucidates the regulation of interface-induced densification and stress segmentation mechanisms by the modulation period during growth and indentation. Subsequently, through subjecting these architectures to different contact pressures, a counter-intuitive pressure-regulated tribological reversal is uncovered. These results demonstrate that the modulation period acts as a kinetic lever, determining whether the film undergoes shear-induced unsaturation or adaptive pressure-densification. It establishes a unified atomistic framework that connects the initial architectural design to the dynamic frictional response.

2. Computational method

2.1. Simulation framework and potential strategy

All MD simulations were performed using the LAMMPS package [17]. To strictly balance computational efficiency with the accuracy of tribochemical reactions, a dual-potential strategy was adopted. The Tersoff potential, optimized for sp^2/sp^3 transitions under varying energies, was employed to describe the deposition process [21,22]. Subsequently, the ReaxFF potential (parameterized by Tavazza et al. [23]) was utilized for the tribological stages. As a bond-order-based field, ReaxFF is essential for capturing the complex bond breaking/formation and interfacial chemistry during the sliding process [24,25]. Especially, to ensure physical consistency, the as-deposited structures were fully relaxed under ReaxFF before friction simulations to minimize artifacts arising from the potential switch. A time step of 0.25 fs was used throughout, with periodic boundary conditions applied in the x and y directions.

2.2. Deposition of modulated DLC films

The deposition substrate consisted of a diamond (001) block ($40.232 \times 40.232 \times 84.779$ Å^3, 3072 atoms), equilibrated at 300 K (Fig. 1). To mimic realistic heat dissipation and structural support, the system was divided into fixed, thermostatic (Berendsen thermostat [26]), and dynamic regions. Carbon atoms were injected from a height of 70 Å with randomized xy coordinates. Based on prior single-energy optimizations [9], multilayer films with 1- to 3-period interfaces were constructed using an alternating energy scheme, with a "hard layer" deposited at 70 eV/atom and a "soft layer" deposited at 1 eV/atom. The atomic ratios and layer thicknesses were tuned to maintain consistent total film thickness across different modulation periods. Sputtered atoms were removed to maintain energy consistency, and post-deposition relaxation was performed at 300 K for 10 ps to ensure structural equilibration.

2.3. Nanoindentation simulation detail

Nanoindentation simulations were performed on the 2×2 expanded supercells of the DLC films using a rigid spherical indenter with a radius of 12 Å. The interaction between the indenter and the film was described by a standard Lennard-Jones (LJ) potential ($\varepsilon = 0.01$ eV, $\sigma = 3.0$ Å) to mimic a purely repulsive contact interface without chemical bonding. The indentation process consisted of three distinct phases: loading, holding, and unloading. During the loading phase, the indenter was driven vertically into the substrate at a constant velocity of 0.5 Å/ps to a maximum penetration depth of 12 Å. Upon reaching the peak depth, a holding period of 20 ps was implemented to allow for structural relaxation, followed by an unloading phase at the same velocity.

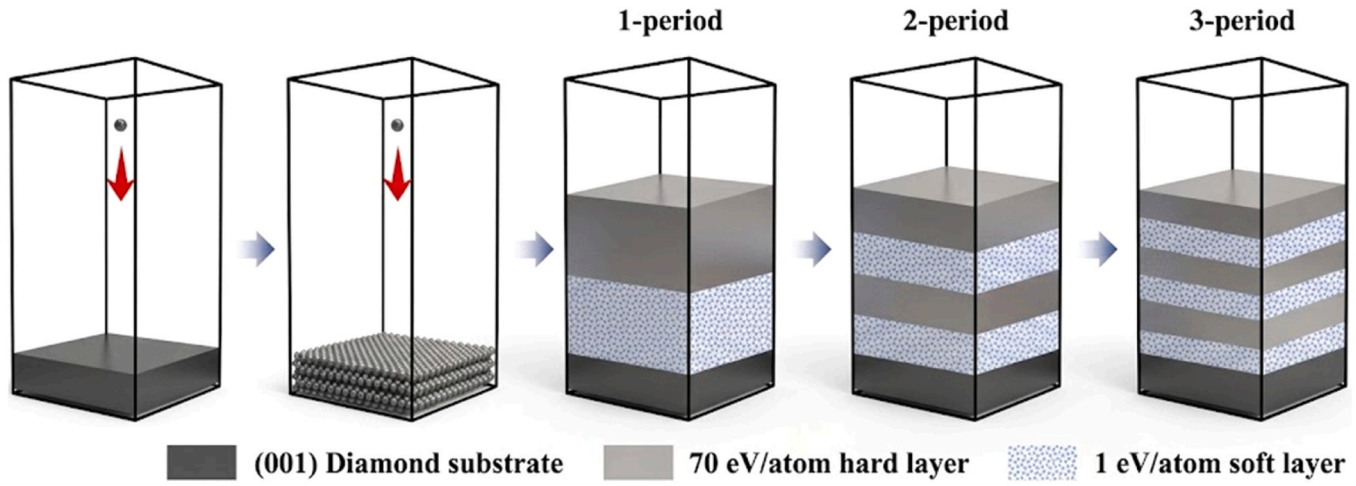

Fig. 1. Schematic illustration of the atomistic deposition strategy for constructing DLC films with distinct periodic modulation architectures on a (001) diamond substrate.

2.4. Tribological Setup and Loading Conditions

A self-mated sliding model was constructed by pairing the deposited DLC films [27]. In line with the deposition phase, the friction system maintained a three-layer configuration consisting of a fixed layer, a thermostatic layer, and a dynamic layer. Tribological tests were conducted under normal contact pressures of 10 and 20 GPa, with a sliding velocity of 100 m/s applied to the top fixed layer along the *x*-direction for 1250 ps. While these parameters exceed macroscopic experimental conditions, they are established standard practices in nanotribology to accelerate tribochemical evolution and ensure sufficient statistical sampling within the nanosecond timescale of MD simulations [28–30]. Specific parameters of the friction process can be found in previous studies [31,32]. The friction coefficient (μ) was calculated as follow:

$$\mu = \frac{f}{W} \tag{1}$$

where the friction force, f, is calculated by summing the force acting on the fixed atoms of the lower a-C model along the sliding direction and W is the normal force acting on the fixed atoms of the lower a-C model along the z direction.

3. Results and discussion

3.1. Morphological characteristics and structural homogenization

The cross-sectional molecular configurations presented in Fig. 2**a** reveal the impact of modulation period on the coordination environment and hierarchical architecture of the DLC films [33]. The 1-period system is characterized by a distinct layered structure, where the carbon network gradually becomes more saturated from the substrate to the surface. However, increasing the number of modulation periods disrupts the layered characteristics and progressively blurs the boundaries between sp^3-dominated and sp^2-dominated regions. This trend suggests that the film architecture evolves from a distinct layered structure into a more intermixed state. This structural evolution originates from the kinetic asymmetry inherent in the energetic deposition process. Carbon atoms at a high incident energy of 70 eV/atom possess sufficient momentum to penetrate deeply into the underlying soft layer. This subplantation effect facilitates strong interlayer bonding but simultaneously creates diffuse and indistinct interfaces. Conversely, low-energy atoms at 1 eV/atom lack the kinetic energy required to infiltrate the dense, hard layer formed previously. This kinetic disparity results in the development of well-defined periodic separation in the 2-period system, where the interfaces remain relatively sharp. Further increasing the modulation period to the 3-period system introduces a competing mechanism driven by sputtering and erosion effects. The frequent bombardment of underlying soft layers by high-energy atoms creates a broad transition region that suppresses the independent growth of pure hard layers. Consequently, the alternating deposition yields a unique quasi-periodic architecture that simultaneously exhibits trends toward structural homogenization.

The stability of these architectural features is further reflected in the surface morphology evolution shown in Fig. 2**b**. While the total film thickness remains constant at approximately 36 Å, the introduction of periodic interfaces significantly influences surface roughness. The 1-period system benefits from the continuous and steady growth of the outermost hard layer and thus maintains a relatively smooth surface profile. In contrast, the frequent interruption of growth by transition regions in the 2-period and 3-period systems hinders the formation of a stable hard cap. This disruption leads to a rougher and more irregular surface morphology as the modulation period increases [14].

The intrinsic structural and mechanical evolutions of the DLC films are quantified by the depth-resolved profiles presented in Fig. 3. These spatial distributions along the z-axis corroborate the morphological

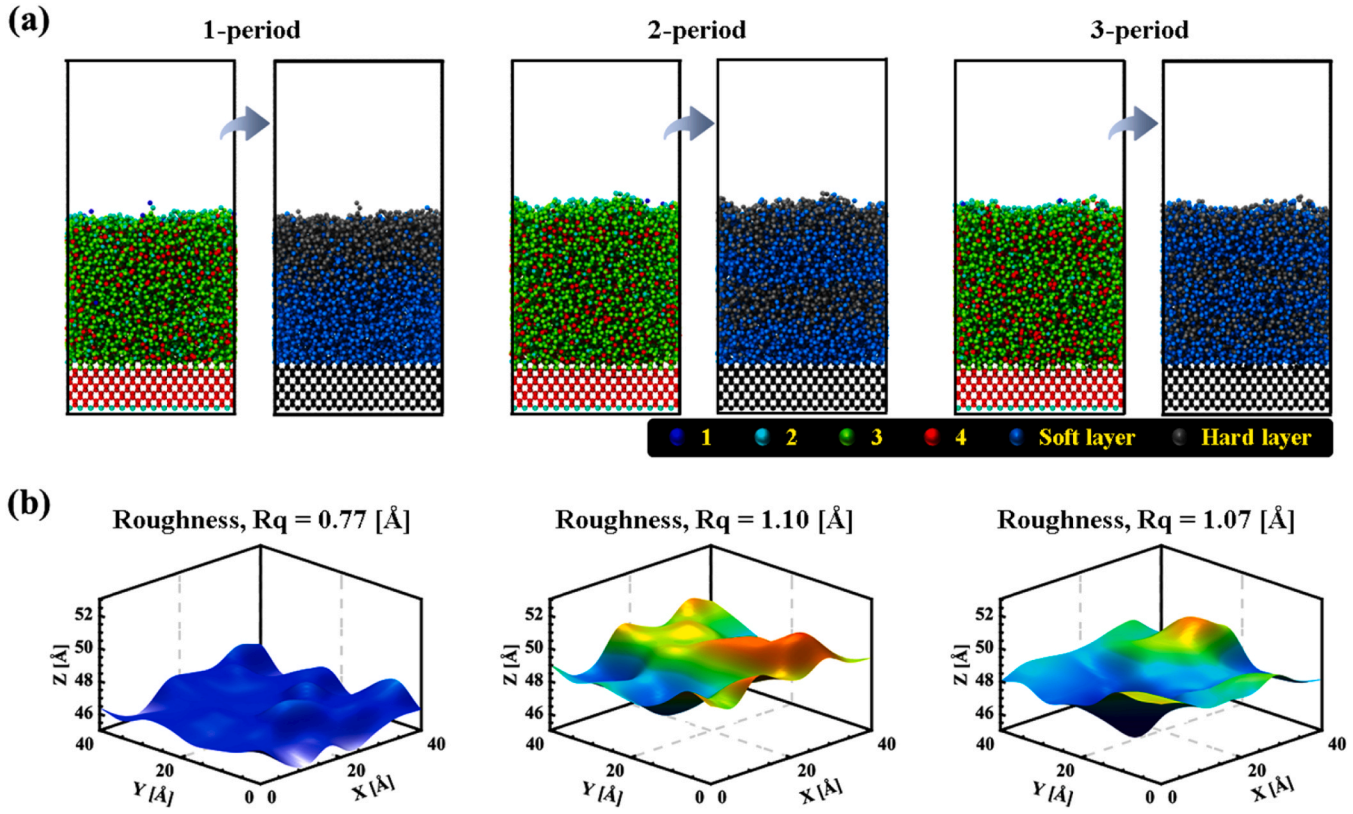

Fig. 2. (a) Coordination configurations of films obtained under different modulation periods. The color coding represents the coordination numbers. (b) Corresponding surface maps and roughness (Rq).

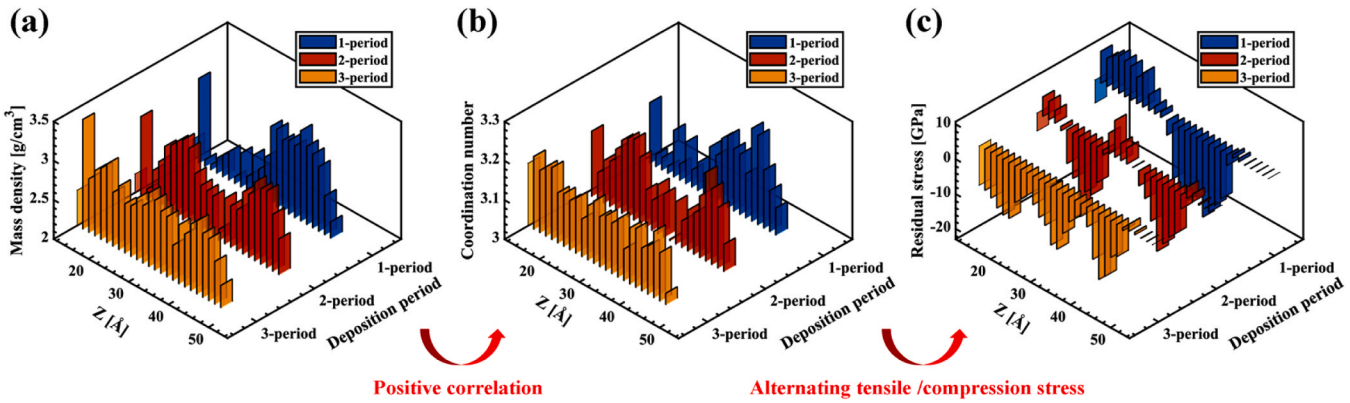

Fig. 3. (a) Density distribution, (b) Coordination distribution, and (c) Residual stress along the *z* direction of DLC films under different modulation periods.

homogenization observed in Fig. 2 and reveal the limitations of increasing modulation period. The amplitude of periodic alternation in both mass density and coordination number significantly attenuates as the number of periods increases. Specifically, the 3-period system exhibits a convergence of soft and hard layer characteristics, implying that the local carbon hybridization no longer maintains a distinct binary separation. Consequently, the film evolves toward a structurally mixed configuration where the intended mechanical contrast between layers is compromised by kinetic intermixing.

A more critical transformation occurs within the residual stress profile (Fig. 3**c**). While the structural composition tends toward homogenization, the internal stress field retains a quasi-periodic oscillation but undergoes a fundamental state shift. The effective stress compensation mechanism observed in the 1-period system, which relies on an

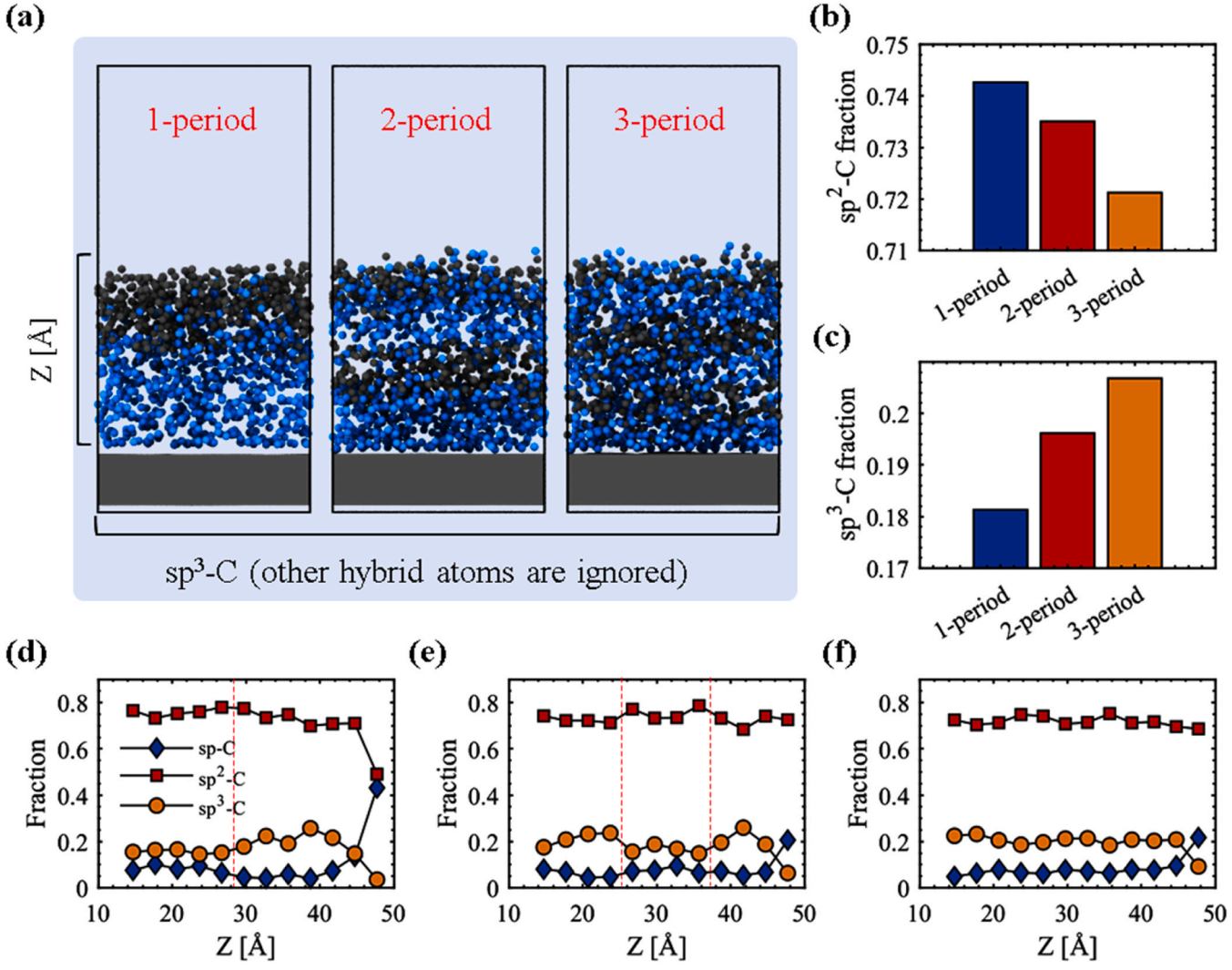

Fig. 4. (a) Visualization of the sp^3 -C backbone architecture. (b, c) Quantitative comparison of hybridization fractions. (d-f) Spatial distribution of bonding states in the 1-period, 2-period, and 3-period systems, respectively.

alternating sequence of tensile and compressive domains, is progressively lost. This pattern transforms into a fluctuation between strong and weak compressive states in the multi-period systems. Such a transition indicates that the structural homogenization induced by frequent interfaces leads to a gradual accumulation of global internal stress rather than the desired compensation [15]. This reveals an intrinsic trade-off in periodically modulated DLC films where the pursuit of finer layering inevitably competes with the capacity for internal stress compensation.

The macroscopic performance of DLC films is fundamentally encoded in the spatial arrangement and relative fractions of sp^3 and sp^2 hybridized carbon atoms. Fig. 4**a** shows how the modulation period reprograms this internal hybridization architecture. The 1-period system maintains a high degree of architectural integrity where distinct soft and hard layers exhibit a sharp contrast in sp^3 density. However, increasing the modulation period induces a progressive structural homogenization. The distinct stratification observed in the 1-period system degrades into a unified network with uniform sp^3 distribution in the 3-period system. This structural convergence suggests that the frequent imposition of high-energy deposition phases actively disrupts the preservation of soft layers. A distinct feature common to all systems is the emergence of a disordered surface layer rich in sp-hybridized carbon. This unsaturated region represents a high-energy surface laden with dangling bonds, which acts as a critical precursor for the subsequent tribochemical interactions.

Quantitative analysis in Figs. 4**b and** 4**c** further reveals that the global fraction of sp^3-C increases positively with the modulation period. In the 1-period system, the thick soft layer partially isolates the underlying structure from high-energy bombardment and allows stable low-density growth. In contrast, the frequent interruption of soft layer growth in multi-period systems exposes these thin regions to intense high-energy carbon subplantation. This energetic impact promotes deep cross-linking and effectively converts potential sp^2 sites into sp^3 configurations through a mechanism of interface-induced densification. Consequently, the modulation period serves as a kinetic lever that dictates the transition from a layered composite to a homogenized high-sp^3 structure.

3.2. *Mechanical response and stress transfer pathways*

The mechanical characteristics of the deposited architectures were evaluated via nanoindentation simulations, as schematically illustrated in Fig. 5**a**. The resulting force-displacement curves in Fig. 5**b** expose a divergence in load-bearing capacity driven by the underlying structural arrangement. The 1-period system displays a distinct mechanical signature characterized by a high initial resistance due to its intact hard cap, followed by a yield behavior as the indenter engages the compliant soft underlayer. This response confirms that the 1-period architecture functions effectively as a composite buffer where the surface layer provides rigidity while the subsurface layer facilitates energy dissipation. In contrast, for the multi-period systems, they display more smooth curves, indicating a stiffer and more monolithic response, which is related to the relatively dense, uniform film structure (Fig. 3 and Fig. 4).

The hardness values derived via the Oliver–Pharr method in Fig. 5**c** rise progressively with the modulation period [34]. This mechanical

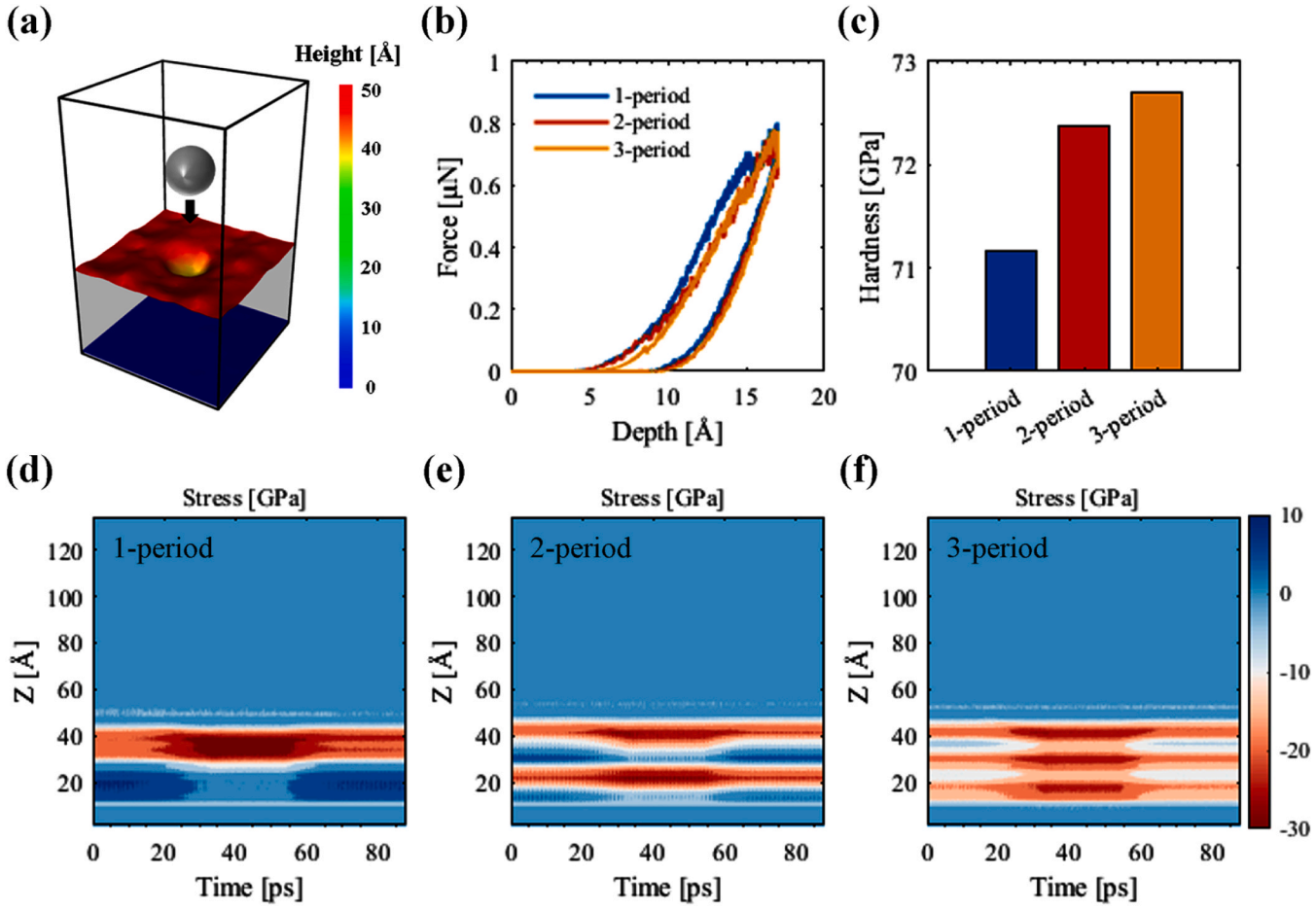

Fig. 5. (a) Schematic of the nanoindentation simulation model used to evaluate the mechanical response of DLC films. (b) Representative force–displacement curves obtained during the loading–unloading process. (c) Hardness. (d–f) Temporal evolution of the internal stress distribution during indentation for the 1-period, 2-period, and 3-period systems, respectively.

reinforcement arises not from the simple stacking of layers, but from the cumulative densification effect driven by the frequent interfaces. The homogenization of the sp^3 network in the 2-period and 3-period systems eliminates the compliant reservoirs required for buffering and results in a global stiffening of the film.

The evolution of internal stress fields presented in Fig. 5**d–f** further clarifies these deformation mechanisms. For the 1-period system, the single thick hard layer exhibits a behavior of monolithic stress concentration. A massive, continuous zone of high compressive stress (indicated by the deep red region) accumulates within this layer. While this confirms its high load-bearing capacity, such concentrated stress accumulation makes the film susceptible to catastrophic failure once the yield limit is exceeded. In contrast, despite the trend toward structural homogenization discussed earlier, the multi-period architectures retain sufficient mechanical contrast to disrupt the stress field. As shown in Figs. 5**e and** 5**f**, the continuous high-stress zone observed in the 1-period system is effectively sliced into multiple discrete strata separated by low-stress bands. These intervening soft layers function as elastic decoupling zones that interrupt the vertical transmission of stress. Consequently, the load is not borne by a single concentrated volume but is distributed across multiple independent hard sub-layers [12]. This transition from localized stress accumulation to distributed multi-stage buffering enhances the ability to manage deformation energy by mitigating peak stress intensity within any single layer, which is difficult to characterize accurately in an experimental approach.

The observed hardness enhancement stems from interface-induced densification, where high-energy subplantation at periodic interfaces converts the soft sp^2 phase into a denser sp^3 network (Fig. 4). This process increases global stiffness but introduces a competition between structural homogenization and phase stability [35]. Consequently, the stress management mechanism shifts from a global buffering mode in the 1-period system to a distributed load-bearing network in multi-period films (Fig. 5). Thus, the governing factor for performance is the maintenance of sharp mechanical contrast, which allows the system to combine high hardness with effective stress segmentation.

In addition, this perspective offers a unified explanation for varying experimental outcomes [13,15]. The successful realization of the stress segmentation mechanism requires a sharp divergence in mechanical properties between the sub-layers. Deposition techniques involving high ionization energies, such as Filtered Cathodic Vacuum Arc (FCVA) [36,37], are capable of generating highly energetic carbon ions. This allows for the deposition of hard layers with exceptionally high sp^3 content and density. Consequently, FCVA-grown films can establish the strong mechanical contrast required to distinguish the soft layers from the hard matrix, thereby activating the stress segmentation effect. In contrast, films produced by conventional magnetron sputtering often suffer from a lower ionization rate and less defined energy control [38,39]. This results in "hard" layers with moderate sp^3 fractions and "soft" layers that lack distinct elasticity. Under such conditions, the mechanical impedance mismatch between layers is insufficient to interrupt stress transmission.

3.3. Tribological response

Building on this understanding of static load-bearing mechanisms, it is imperative to further investigate whether the observed benefits of stress segmentation and mechanical contrast translate into superior tribological performance under dynamic sliding conditions. This is achieved by fabricating the self-mated sliding model, illustrated in Fig. 6**a** for friction simulation, and according to the modulated period of DLC film (1-period (p1), 2-period (p2), and 3-period (p3)) and applied contact pressures (10 and 20 GPa), the friction system is abbreviated as p1–10, p1–20, p2–10, p2–20, p3–10, and p3–20, respectively, for convenience.

Upon the initiation of sliding, all systems undergo a characteristic running-in phase before converging to a dynamic steady state as shown in Fig. 6**b**. Despite the overlap in the instantaneous friction traces, a distinct pressure-dependent reversal in friction is uncovered by the quantitative analysis of the final 200 ps presented in Fig. 6**c and** Fig. S1. Under the moderate contact pressure of 10 GPa, the friction coefficient exhibits a positive correlation with the modulation period, which increases progressively from the 1-period to the 3-period system (Fig. 6**c**). This trend originates from the load-bearing limitations observed in Fig. S1b, where the normal load capacity diminishes with increasing periods. This suggests that at lower contact pressures, the numerous soft interlayers in the multi-period systems act as structural weak points that yield under load rather than supporting the film integrity.

In contrast, increasing the contact pressure to 20 GPa triggers a complete reversal of this trend. The friction coefficient decreases as the number of modulation periods increases (Fig. 6**c**). This transition indicates that the high-pressure environment activates the interface-induced densification mechanism discussed previously. Under these conditions, the multi-period architectures undergo rapid homogenization and hardening, which allows them to support higher normal loads (Fig. S1b) while simultaneously reducing shear resistance (Fig. S1a). Consequently, the modulation period functions as a critical switch that dictates the tribological regime. It shifts the system from a shear-dominated state where interfaces are liabilities to a pressure-dominated state where interface-induced densification minimizes friction. This reversal should not be attributed to real contact area,

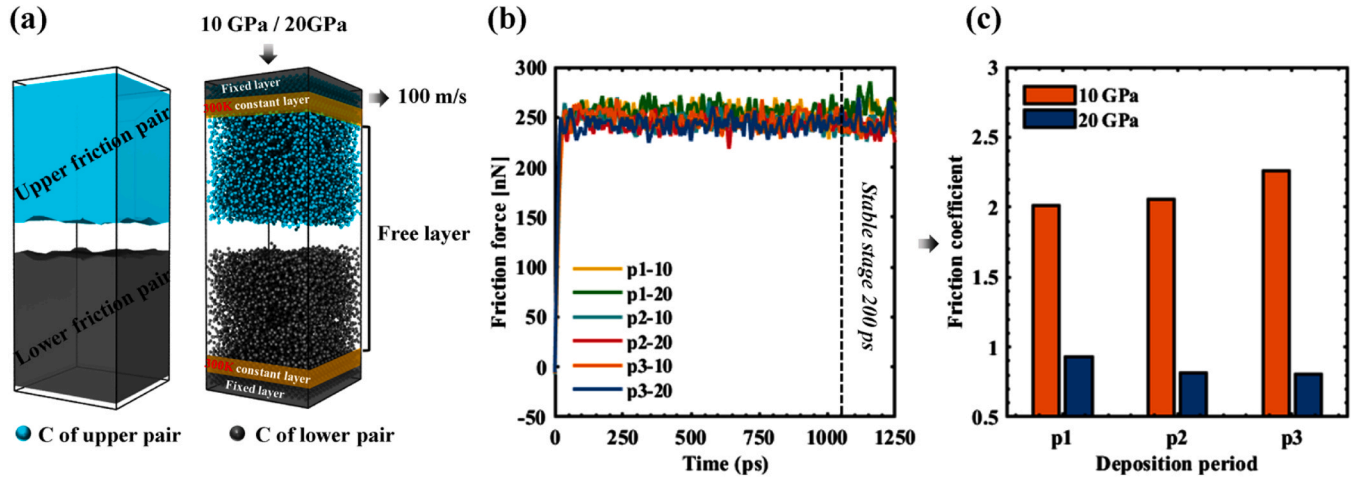

Fig. 6. (a) Friction pair constructed from the deposited DLC films. (b) Temporal evolution of friction forces during sliding. (c) Friction coefficient of different deposition systems.

interfacial bonding, or load-bearing capacity alone (Fig. S1), because these factors are strongly coupled with the pressure-dependent hybridization evolution of the interfacial carbon network. At 10 GPa, the interface evolves toward disordered sp^2-rich carbon with higher shear resistance, whereas at 20 GPa, enhanced C–C bonding promotes the formation of a compact sp^3-rich tribofilm with improved load-bearing stability, as will be discussed in detail below.

The temporal evolution of mass density maps before and after sliding processes reveals a progressive structural transformation in the p2–10 system under shear (Fig. 7**b**). The initially distinct density stripes, which correspond to the soft and hard layers, gradually smear out into a more continuous distribution (Fig. 7**a**). This blurring signifies a shear-induced mixing process, wherein sliding promotes atomic diffusion across the interfaces. Correspondingly, the stress field transitions from a stratified state to a uniformly compressive distribution, as confirmed by the data in Fig. 7**c**. A layer-resolved analysis of the final density profiles further elucidates the homogenization mechanism under 10 GPa. The structural integrity is inversely related to the modulation period, with the p1–10 system maintaining a sharp interface between its densified soft layer and shear-loosened hard layer (Fig. 7**d**). In multi-period systems, however, significant peak broadening occurs (Figs. 7**e and** 7**f**). The p3–10 system, in particular, exhibits extensive density overlap, indicating that its thin soft layers cannot withstand shear and succumb to interfacial cross-linking (Fig. 7**f**).

However, at 20 GPa, the system enters a pressure-dominated densification regime. The density evolution maps in Fig. S2 reveal that the periodic low-density stripes visible at 10 GPa are almost entirely eliminated at 20 GPa. Instead, the entire film volume evolves into a high-density state characterized by a pervasive red coloration in the color maps. This observation is further supported by Fig. S3, which presents the layer-resolved density distributions for the p1–20, p2–20, and p3–20 systems. Unlike the clearly separated peaks observed at 10 GPa, the profiles at 20 GPa indicate that even the originally soft layers become compacted to densities comparable to those of the hard layers. This ubiquitous densification explains the friction reversal observed earlier. Under high pressure, the soft buffering layers are effectively forged into a hard tribofilm. This creates a homogenized and stiff interface with improved load-bearing stability, thereby reducing the effective shear resistance despite the loss of the original modulation architecture.

The tribological mechanisms are fundamentally governed by the dynamic evolution of interfacial connectivity. For the subsequent analysis of interfacial bonding and hybridization evolution, the friction interface is defined as the structurally mixed contact region between the two opposing DLC surfaces, where pronounced density variation and shear-induced atomic mixing occur during sliding process. At 10 GPa, Fig. 8**a** reveals a distinct shear-driven rehybridization process. The friction surfaces are initially populated by abundant unsaturated sp-hybridized terminations. Upon sliding process, shear stress forces these segments to bridge with the counter-surface and rapidly consumes the unstable sp species to form a cross-linked sp^2 network. In contrast, the system at 20 GPa exhibits a state of pressure-enhanced saturation. As shown in Figs. 8**b and** 8**c**, the interface maintains a consistently high coordination density throughout the sliding process. This indicates that the high contact pressure instantly compresses the interface into a dense network where stable covalent bonds predominate from the onset without requiring a gradual accumulation phase.

The increased C-C bonding in Fig. 8**d** confirms the difference in this mechanism. The significantly faster and more extensive C–C bond formation at 20 GPa validates the existence of a pressure-saturated regime where the carbon network is actively forged into a dense tribofilm. This highly saturated structure minimizes reactive dangling bonds and effectively lowers shear resistance. Consequently, the tribological behavior shifts from a regime governed by the shear-induced consumption of sp sites at 10 GPa to a regime dominated by pressure-

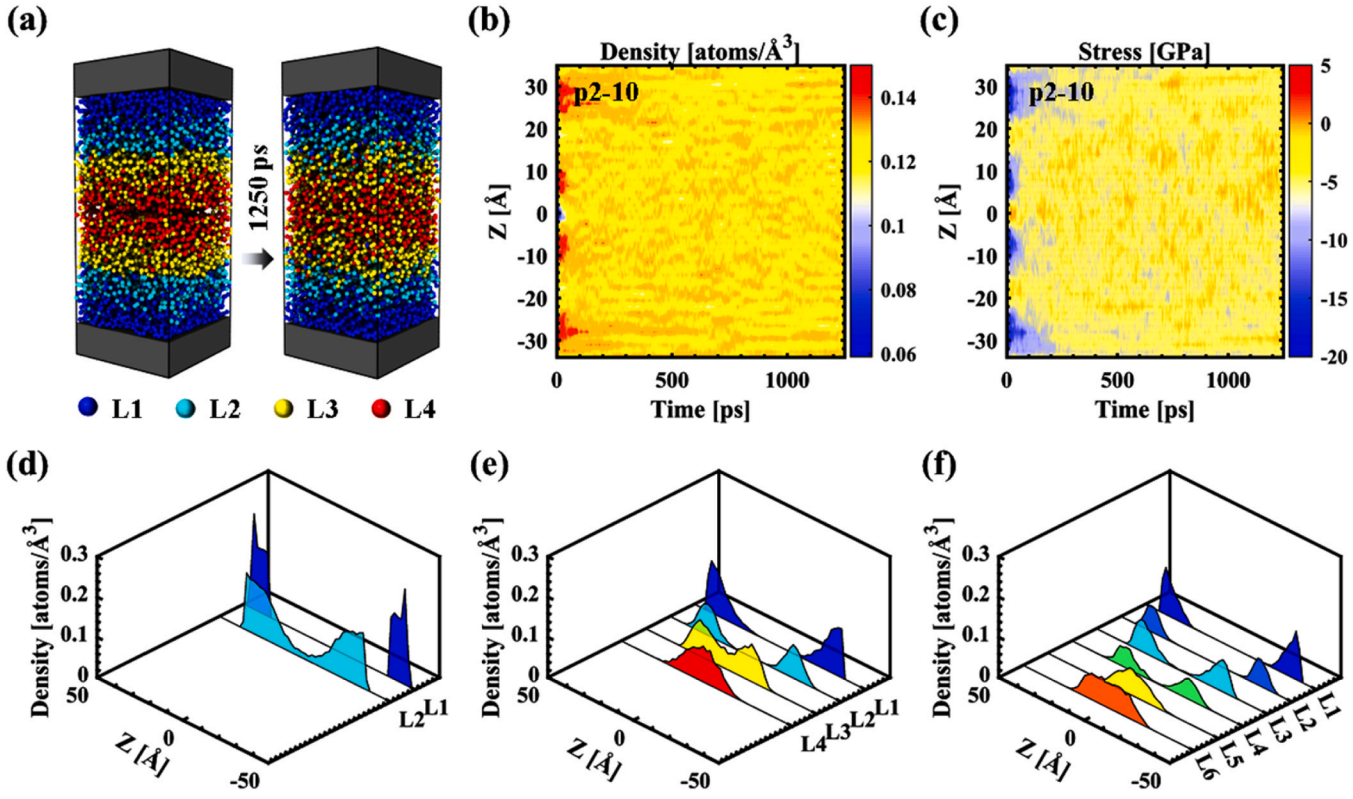

Fig. 7. (a) Layered morphology of the p2−10 system before and after sliding processes. (b) Density evolution of the p2−10 system during the sliding process. (c) Stress evolution of the p2−10 system during the sliding process. (d–f) Layer-resolved density distributions at the end of the sliding process for the p1−10, p2−10, and p3−10 systems, respectively.

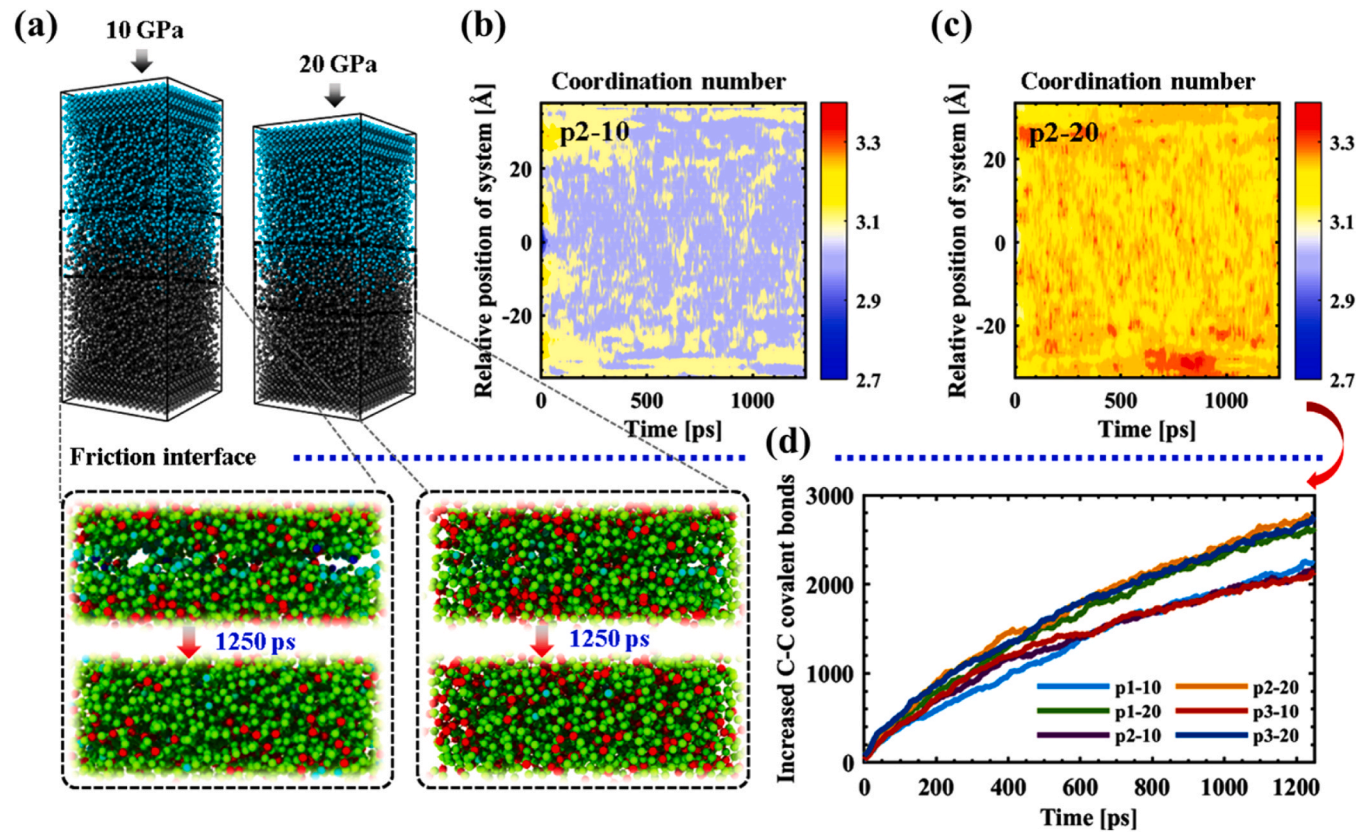

Fig. 8. (a) Original morphology of the p2−10 and p2−20 systems before the sliding process, in which the enlarged ones are the coordination morphologies of the friction interface before and after friction processes. (b) Coordination number distribution during the friction process for the p2−10 system. (c) Coordination number distribution during the friction process for the p2−20 system. (d) Increase in C–C covalent bonding as the coordination number grows during the friction process.

stabilized saturation at 20 GPa.

A deeper examination of the hybridization changes associated with interfacial bonding provides crucial insight into the mechanisms governing the friction coefficient. As shown in Fig. 9, together with Figs. S4 and S5, all systems exhibit a trend toward structural homogenization where the initial layering boundaries fade during the sliding process. However, the hybridization transition is strictly governed by the contact pressure.

At 10 GPa, the system exhibits a shear-dominated structural transformation. As shown in **Figs. 9a, S4a, and S5a**, the sp^3 fraction decreases markedly over the sliding process while the sp^2 fraction rises. This trajectory indicates that the applied shear stress destabilizes the rigid sp^3 network and promotes a transformation toward a softer sp^2-rich configuration (Fig. 9**c**). The multi-period systems, particularly p3–10, possess a thinner surface monolayer that is kinematically unstable against shear mixing. This structural softening diminishes the load-bearing capacity of the interface and increases the effective shear resistance, which is reflected by the higher friction coefficient of the multi-period films (Fig. 6**c and** Fig. S1). Conversely, the p1–10 system retains a thick and robust hard surface layer (Fig. S4a) that resists shear-induced unsaturation and thus maintains lower friction.

In contrast, increasing the pressure to 20 GPa activates a pressure-driven densification regime. The hybridization distributions in **Figs. 9b, S4b, and S5b** show that sp^3 hybridized species accumulate significantly during the sliding process, while the proportion of sp^2 hybridized species tends to stabilize or decrease. This trend confirms that high compressive stress actively forces the conversion of unsaturated carbon into dense sp^3 bonding. The multi-period architectures contain numerous soft interfaces that serve as fertile sites for this pressure-induced transformation. The modulation period functions as an asset for adaptive hardening under high pressure. The stress dispersion mechanism in nanoindentation also demonstrates that multi-period systems are better adapted to high-pressure environments. The p3–20 system exhibits the most dramatic increase in sp^3 fraction in Fig. 9**c** because its abundant soft material is effectively forged into a hard tribofilm. The p1–20 system, being initially saturated, lacks this adaptive capacity and shows minimal structural enhancement.

Therefore, the tribological behavior of modulated DLC films is defined by a critical pressure threshold that separates shear-induced softening from pressure-induced hardening. The modulation period determines the sensitivity of the film to these regimes. High modulation period accelerates structural unsaturation at low pressures but facilitate rapid adaptive densification at high pressures. This fundamental mechanism explains the frictional crossover and suggests that the optimal design of multilayer architectures must be tailored to the specific contact pressure of the intended application. Although the simulated film thickness is much smaller than that of practical DLC films, the pressure-dependent structural evolution identified here occurs mainly within the near-surface contact region and can therefore provide atomistic guidance for thicker multilayer films.

4. Conclusion

This study has systematically explored the atomistic mechanisms governing the mechanical and tribological responses of periodically modulated DLC films via large-scale MD simulations. By linking the kinetic deposition to the in-situ structural evolution under different contact pressures, this work establishes a unified atomistic theoretical framework for modulated DLC films. The key conclusions are summarized as follows:

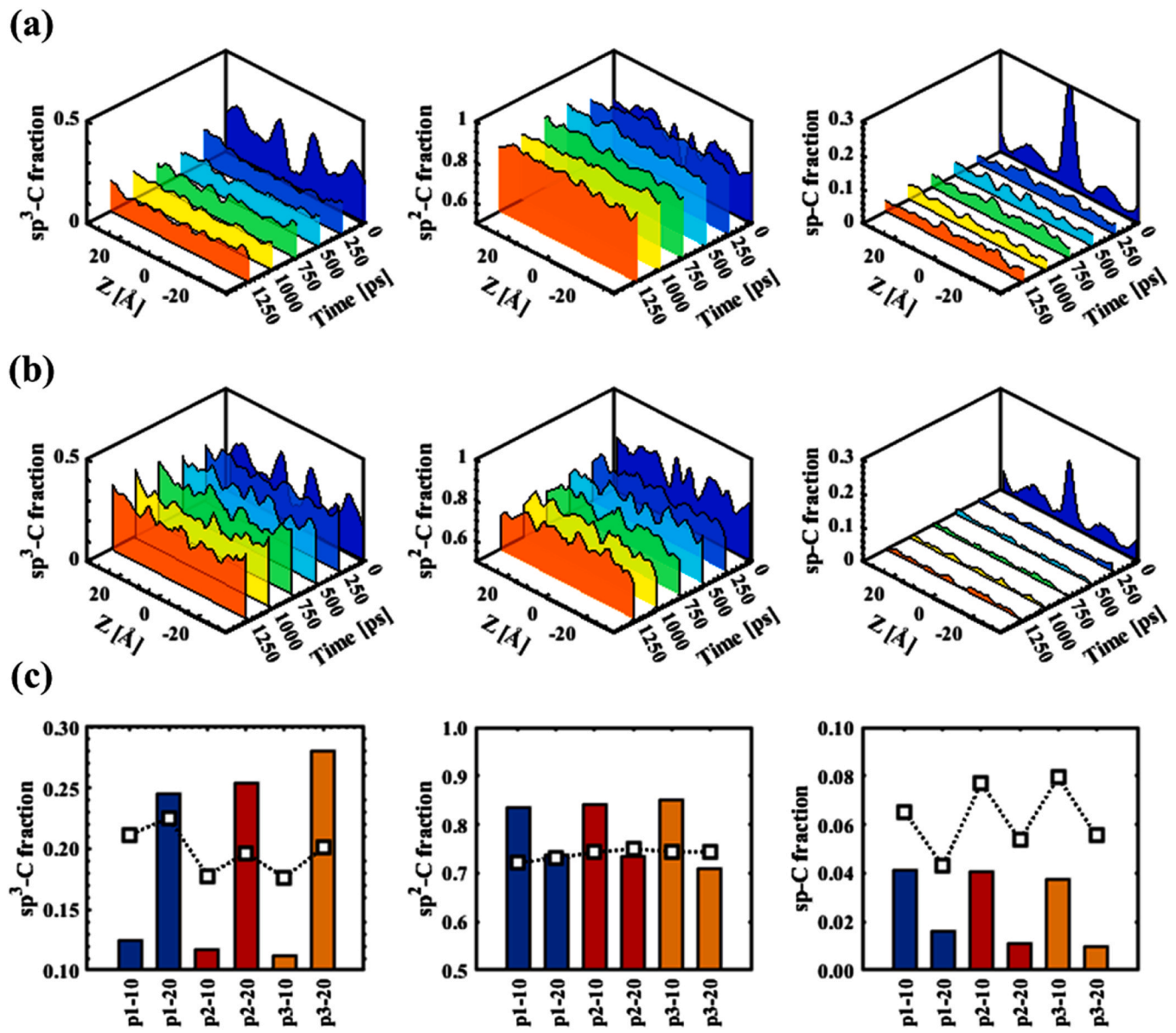

Fig. 9. Distributions of hybridized structures in the (a) p2−10 and (b) p2−20 systems, respectively, during the sliding process. (c) Hybridized structure at the friction interface before and after sliding processes (dotted line represents pre-sliding result, bar graph represents post-sliding result.).

- The modulation period is not merely a geometric parameter but a determinant of film quality. Frequent high-energy bombardment at periodic interfaces drives an in-situ densification of the soft layers, enhancing the global sp^3 fraction and hardness. Mechanically, the multilayer architecture transforms the stress dissipation mode from "monolithic buffering" in single-period films to "distributed stress segmentation" in multi-period systems. The surviving soft interlayers segment peak stress accumulation into manageable discrete zones, thereby preventing catastrophic failure while maintaining load-bearing capacity.
- A fundamental crossover in frictional behavior governed by contact pressure is identified. At 10 GPa, the friction coefficient increases with modulation period, whereas at 20 GPa, this trend is completely reversed, with multi-period systems exhibiting the lowest friction. These findings highlight that the "optimal" period is not an intrinsic property but is strictly dependent on the operational load regime.
- The frictional reversal originates from the competition between shear-induced softening and pressure-induced densification. At 10 GPa, high-frequency modulation promotes shear-driven disordering and sp^2-rich structural evolution, which increases the effective interfacial shear resistance. In contrast, at 20 GPa, high compressive stress facilitates the formation of a compact and saturated sp^3-rich tribofilm, improving load-bearing stability and reducing shear resistance.
- These findings suggest that multilayer DLC films should be designed according to their specific service conditions. For high-pressure contacts, increasing the modulation period can activate pressure-induced densification and improve tribological performance. For lower-pressure conditions, preserving thicker and more stable layers is more favorable for resisting shear-induced degradation. This work provides atomistic guidance for designing load-adaptive carbon-based coatings.

CRediT authorship contribution statement

Xubing Wei: Writing – original draft, Formal analysis. **Rende Chen:** Writing – original draft, Formal analysis. **Xinmeng Wu:** Writing – original draft, Formal analysis. **Meng Cheng:** Writing – original draft,

Formal analysis. **Peng Guo:** Writing – original draft, Formal analysis. **Kwang-Ryeol Lee:** Writing – review & editing, Supervision, Resources, Conceptualization. **Aiying Wang:** Writing – review & editing, Supervision, Conceptualization. **Naizhou Du:** Writing – original draft, Visualization, Methodology, Investigation, Formal analysis, Data curation, Conceptualization. **Qiaoyun Dong:** Writing – original draft, Formal analysis. **Weidong Dang:** Writing – original draft, Formal analysis. **Xinlin Zhao:** Writing – original draft, Formal analysis. **Xiaowei Li:** Writing – review & editing, Writing – original draft, Supervision, Resources, Investigation, Funding acquisition, Data curation, Conceptualization.

Declaration of Competing Interest

The authors declare that they have no known competing financial interests or personal relationships that could have appeared to influence the work reported in this paper.

Acknowledgments

This research was supported by the National Natural Science Foundation of China (No. U24A2030), Xuzhou "343" Industrial Development Project (No. gx2025006), Science and Technology Project of Zhejiang Province (No. 2026C02A1253(SD2)) , and Natural Science Foundation of Ningbo (No. 2024Z134, No. 2025QL023).

Appendix A. Supporting information

Supplementary data associated with this article can be found in the online version at doi:10.1016/j.triboint.2026.112370.

Data availability

Data will be made available on request.

References

[1] Robertson J. Diamond-like amorphous carbon. Mater Sci & Eng R-Rep 2002;37(4-6):129–281.
[2] Bewilogua K, Hofmann D. History of diamond-like carbon films - From first experiments to worldwide applications. Surf & Coat Technol 2014;242:214–25.
[3] Abadias G, Chason E, Keckes J, et al. Review Article: Stress in thin films and coatings: Current status, challenges, and prospects. J Vac Sci & Technol A 2018;36(2):020801.
[4] Lei Y, Jiang J, Wang Y, et al. Structure evolution and stress transition in diamond-like carbon films by glancing angle deposition. Appl Surf Sci 2019;479:12–9. 12-19.
[5] Podsvirov OA, Karaseov PA, Vinogradov AY, et al. Residual stress in diamond-like carbon films: Role of growth conditions and ion irradiation. J Surf Investig 2010;4(2):241–4.
[6] Zhu L, Li J, Kang J, et al. Different Cr contents on the microstructure and tribomechanical properties of multi-layered diamond-like carbon films prepared by unbalanced magnetron sputtering. J Mater Eng Perform 2020;29(11):7131–40.
[7] Ahmed N, Khan ZS, Ali A. Microstructure and residual stress dependence of molybdenum films on DC magnetron sputtering conditions. Appl Phys A-Mater Sci & Process 2022;128(11):967.
[8] Kabir MS, Zhou Z, Xie Z, et al. Designing multilayer diamond like carbon coatings for improved mechanical properties. J Mater Sci & Technol 2021;65:108–17.
[9] Du N, Wang Y, Wei X, et al. Low-stress optimization and enhanced tribological properties of multilayer DLC films via alternating-energy deposition. Carbon 2025;244:120721.
[10] Zhao Y, Xu F, Yuan L, et al. Microstructural, mechanical and tribological performances of DLC/CrN multilayer films with different modulation period. Diam Relat Mater 2025;154:112163.
[11] Wei J, Li H, Liu L, et al. Enhanced tribological and corrosion properties of multilayer ta-C films via alternating sp3 content. Surf & Coat Technol 2019;374:317–26.
[12] Wang J, Pu J, Zhang G, et al. Interface architecture for superthick carbon-based films toward low internal stress and ultrahigh load-bearing capacity. ACS Appl Mater & Interfaces 2013;5(11):5015–24.
[13] Xu Z, Zheng YJ, Jiang F, et al. The microstructure and mechanical properties of multilayer diamond-like carbon films with different modulation ratios. Appl Surf Sci 2013;264:207–12.
[14] Lin Y, Zhou Z, Li KY. Improved wear resistance at high contact stresses of hydrogen-free diamond-like carbon coatings by carbon/carbon multilayer architecture. Appl Surf Sci 2019;477:137–46.
[15] Usman M, Zhou Z, Zia AW, et al. Designing hydrogen-free diamond like multilayer carbon coatings for superior mechanical and tribological performance. Tribology Int 2024;192:109211.
[16] Lin Y, Zia AW, Zhou Z, et al. Development of diamond-like carbon (DLC) coatings with alternate soft and hard multilayer architecture for enhancing wear performance at high contact stress. Surf Coat Technol 2017;320:7–12.
[17] Thompson AP, Aktulga HM, Berger R, et al. LAMMPS - a flexible simulation tool for particle-based materials modeling at the atomic, meso, and continuum scales. Comput Phys Commun 2022;271:108171.
[18] Du N, Li X, Wei X, et al. Atomistic Insights into Interfacial Optimization Mechanism for Achieving Ultralow-Friction Amorphous Carbon Films under Solid–Liquid Composite Conditions. ACS Appl Mater & Interfaces 2023;15(45):53122–35.
[19] Wei X, Du N, Guo P, et al. Friction dependence on processing priority for graphitization/passivation coupled amorphous carbon films. Carbon 2024;230:119631.
[20] Wang P, Yang X. Elucidating deposition process of calcium carbonate and mechanical properties of precipitation via molecular dynamics simulation. Surf Interfaces 2024;49:104460.
[21] Li X, Ke P, Zheng H, et al. Structural properties and growth evolution of diamond-like carbon films with different incident energies: A molecular dynamics study. Appl Surf Sci 2013;273:670–5.
[22] Li X, Ke P, Lee K, et al. Molecular dynamics simulation for the influence of incident angles of energetic carbon atoms on the structure and properties of diamond-like carbon films. Thin Solid Films 2014;552:136–40.
[23] Tavazza F, Senftle TP, Zou C, et al. Molecular Dynamics Investigation of the Effects of Tip–Substrate Interactions during Nanoindentation. J Phys Chem C 2015;119(24):13580–9.
[24] Li X, Wang A, Lee K. Fundamental understanding on low-friction mechanisms at amorphous carbon interface from reactive molecular dynamics simulation. Carbon 2020;170:621–9.
[25] Li X, Xu X, Zhou Y, et al. Insights into friction dependence of carbon nanoparticles as oil-based lubricant additive at amorphous carbon interface. Carbon 2019;150:465–74.
[26] Berendsen HJC, Postma JPM, van Gunsteren WF, et al. Molecular dynamics with coupling to an external bath. J Chem Phys 1984;81(8):3684–90.
[27] Li X, Wang A, Lee K. Mechanism of contact pressure-induced friction at the amorphous carbon/alpha olefin interface. npj Comput Mater 2018;4(1):53.
[28] Ma T, Wang L, Hu Y, et al. A shear localization mechanism for lubricity of amorphous carbon materials. Sci Rep 2014;4(1):3662.
[29] Corni S, Righi MC, Zilibotti G. Load-Induced Confinement Activates Diamond Lubrication by Water. Phys Rev Lett 2013;111(14):146101.
[30] Xiao N, Tang J, Zhou S, et al. Current research on the design, properties and applications of tribological materials: a review. RSC Adv 2025;15(41):34669–717.
[31] Du N, Feng C, Chen K, et al. Friction dependence on the textured structure of an amorphous carbon surface: A reactive molecular dynamics study. Appl Surf Sci 2023;610:155584.
[32] Du N, Li X, Wei X, et al. Comprehensive optimization of friction performance of amorphous carbon films under complex solid–liquid composite conditions. Appl Surf Sci 2025;688:162468.
[33] Stukowski A. Visualization and analysis of atomistic simulation data with OVITO–the Open Visualization Tool. Model Simul Mater Sci Eng 2010;18(1):15012.
[34] Zhou Y, Ding M, Niu X, et al. Molecular dynamics investigation of metastable structure and hybridization bond evolution in high-entropy CoCrFeNi heterostructured amorphous carbon Films. Langmuir 2024;40(34):18242–53.
[35] Wang L, Zhang Z, Chen H, et al. Friction behavior of diamond-like carbon coatings with different sp3 contents by atomistic-scale friction dynamics. Surf Coat Technol 2023;464:129580.
[36] Wei J, Guo P, Li H, et al. Insights on high temperature friction mechanism of multilayer ta-C films. J Mater Sci & Technol 2022;97:29–37.
[37] Xu S, Li X, Huang M, et al. Stress reduction dependent on incident angles of carbon ions in ultrathin tetrahedral amorphous carbon films. Appl Phys Lett 2014;104(14):141908.
[38] Sarakinos K, Alami J, Konstantinidis S. High power pulsed magnetron sputtering: A review on scientific and engineering state of the art. Surf Coat Technol 2010;204(11):1661–84.
[39] Kubart T, Aijaz A, Andersson J, et al. High power impulse magnetron sputtering of diamond-like carbon coatings. J Vac Sci & Technol A 2020;38(4):43408.